



ISSN 1110-0451



(E S N S A)

Trace Elements Characterization in Rocks Using Neutron Activation Analysis, Northwestern Coast, Ras El-Hekma–Egypt

A. Massoud¹, Fatma S. Adou², M. Youssif³, Wael. M. Badawy^{4,5}, K. F. Allan¹

¹Nuclear Chemistry Department, Hot Labs Center, Egyptian Atomic Energy Authority (EAEA), P.O. 13759, Cairo, Egypt

²Reactor Physics Department (Egypt Second Research Reactor), Nuclear Research Centre, Egyptian Atomic Energy Authority, P.O. Box 13759, Inshas, Cairo, Egypt

³Geology Department, Desert Research Center, P.O. Box 11753, El Matariya, Cairo, Egypt

⁴Radiation Protection Department, Nuclear Research Centre, Egyptian Atomic Energy Authority, Cairo, Egypt

⁵Frank Laboratory of Neutron Physics, Joint Institute for Nuclear Research, 141980 Dubna, Russian Federation

ARTICLE INFO

Article history:

Received: 12th Oct. 2023

Accepted: 22nd Jan. 2024

Available online: 7th Mar. 2024

Keywords:

rock samples;

neutron activation analysis
NAA;

trace elements;

multivariate statistical
analysis;

enrichment.

ABSTRACT

The current work was carried out to characterize rock samples of mudstone, sand, and limestone collected at different depths from Northwestern Coast, Ras El-Hekma – Egypt. The samples were subjected to neutron activation analysis to determine the elemental composition and to better understand the geochemistry of the rocks. The abundance of 17 elements was determined. Bivariate and multivariate statistical analyzes were performed to investigate the origin of rocks and common geochemical characteristics (i.e., type, origin, geological history, major and trace composition, weathering, and alteration). The normalized results obtained showed that the abundances of Ca and Sr were significant compared to the corresponding values in the literature. The enrichment factor (EF) was calculated to obtain more information about the sources of the increased abundances of the metals. The results obtained can provide baseline data for the surveyed region and can be utilized by the government, policymakers, and interested parties for future research and development endeavors and planning.

1. INTRODUCTION

The elemental composition of rock samples from various depths has been studied extensively in recent years to understand the environmental factors (temperature, pressure, rock type, weathering, geological processes, human activity...etc) that influence the distribution of elements in the Earth's crust [1]. The analysis of sedimentary rock samples can provide valuable insight into the geologic history of a region, and the study of the elemental composition of rock samples at different depths can improve the understanding of the geology of the area [2-4].

Different elements are associated with different geological processes, and the variation in the elemental composition of rock samples at different depths can inform us about the various chemical, physical and biological processes that have contributed to the

formation of the rock. Furthermore, the elemental composition of rock samples at different depths is also influenced by the processes of sedimentation and erosion.

Sedimentation can lead to the accumulation of heavier elements in the lower portions of the crust, while erosion can lead to their removal [5]. In this regard, the present work will shed light on the characterization of different rock samples that were collected at various depths in terms of the elemental association.

In addition, the provenance (composition of the rocks from which fine-grained sediments formed) and subsequent interactions with fluids, which convert these source rocks into solutes and newly formed minerals in the surface environment, are the primary factors governing the elemental composition of fine-grained sediments (weathering). Furthermore, as reported by

Lipp, Shorttle, Syvret, and Roberts [5], determining how each of these elements contributed to the production of a particular sediment is a difficult task for sedimentary geochemistry. Then, by analyzing the elemental compositions of sedimentary layers, it is possible to learn important facts about former climatic conditions, crustal processes, and sedimentary source areas. Eventually, major and trace element data provide constraints on both the provenance composition and the effects of sedimentary processes, such as weathering and sedimentary sorting [6]. To elucidate the provenance of different rocks, understanding elemental ratios is one of the most important aspects of rock classification. The most used elemental ratio indicators are aluminum-silicon, calcium-magnesium, and silicon-magnesium. The aluminum-silicon ratio is a key indicator of the magma's origin and the type of rock it will form after cooling. Low aluminum-silicon ratios indicate that the magma cooled slowly and produced intrusive igneous rocks, such as granite and gabbro. High aluminum-silicon ratios indicate that the magma cooled quickly and produced extrusive igneous rocks, such as basalt and andesite. Calcium-magnesium ratio indicates the relative amounts of these two elements in the magma [7, 8]. Magma with low calcium-magnesium ratios is more acidic, indicating it will form silica-rich rocks such as rhyolite and dacite. Magma with high calcium-magnesium ratios is more basic, indicating it will form calcium-rich rocks such as dolerite and gabbro [9, 10].

It was proved by other authors that the elemental composition of sedimentary rock samples can vary greatly depending on the depth. At the surface, the main elements found in sedimentary rock samples are typically Fe, Na, Al, Ca, K, and Mg [11], while subsurface samples typically contain Ca, Fe, Al, and other elements [10]. This is because the elemental composition of sediment is set by the composition of its protolith and can be further modified by weathering, sorting, and diagenesis [5].

In this regard, conventional statistical techniques cannot be applied to the compositional data of rocks and if such techniques are used on raw data, the results can be misleading [12]. Consequently, centered log-ratio transformations (CLR) are a practical method for handling compositional data. Standard statistical methods can be used more successfully by converting the data into a log-ratio space. Once compositional data are transformed into log-ratio space, simple linear trends can be used to predict geological processes, for example, weathering, sorting,

and igneous differentiation [13]. Based on that, the obtained compositional data of the elements will be statistically treated before the implementation of various multivariate statistical analyses.

Many techniques by destructive procedures such as ICP-AES, ICP-MS, Atomic Absorption, and UV, have been used to determine the elemental compositions in the solid samples [14-29]. Neutron activation analysis (NAA) stands out among the highly precise and sensitive analytical methods currently in use in that it does not require prior sample preparation, such as acid digestion, which greatly improves both precision and accuracy in determining the content of major and trace elements in rocks [3, 30]. Neutron analysis and appropriate statistical methods were used to investigate the extent to which the elemental composition of different rocks varies at different depths even when the rock type is the same. The current study focused on an area called Ras El-Hekma for several reasons. Firstly, the Egyptian government is making significant investments in developing new villages and towns along the northwestern coast, which makes it a relevant area to study. Additionally, Ras El-Hekma is a major tourist destination on the northwest coast.

The primary goals of the current work can be summed up as follows; i) determining the elemental composition of major and trace elements in selected rock samples from Ras El-Hekma region - Egypt; ii) studying the distribution patterns of the obtained elements at different depths; iii) implementation of ratio indicators for rock classification and provenance; iv) identification of enriched metal rocks using enrichment factor; and eventually v) applying multivariate statistical analysis to extract more information about the common geochemical features of rocks based on metal content.

2. Materials and methods

2.1. Features of the studied area

Ras El-Hekma is located on the northwest coast of Egypt, about 70 km east of Matrouh City (27° 48' 26.1'' E and 31° 03' 59.2'' N), and looks directly onto the Mediterranean Sea, as can be seen in Figure 1. Being Located on the northwest coast of Egypt, Ras El-Hekma is a popular destination for tourists who want to enjoy the beautiful scenery, serene atmosphere, and sandy beaches. The area's strategic location also makes it an important area to study and analyze, given the ongoing developments by the Egyptian government to create new villages and towns along the coast.

2.2. Geological setting

Based on field studies of the geological map and works of Yousif and Bubenzler [31, 32] the geologic exposures on the surface of the study area can be differentiated from older to younger as follows: (a) Neogene deposits are exposed in the southern parts of the study area, where they are represented by Pliocene sediments, which are exposed to a limited extent, and Middle Miocene sediments (Marmarica limestone formation). The middle Miocene consists of fractured and cavernous limestone, dolomitic, and sandy limestone intercalated with clay and marl. (b) Pleistocene sediments are also widely distributed in the study area and consist of oolitic limestone. (c) Holocene sediments are along the

beach and are composed of matured sand and contain some fine clayey and/or calcareous particles. These rock units are also recorded in the subsurface, in addition to the Lower Miocene deposits which do not have any exposures on the surface (only recorded in the drilled wells) [31].

2.3. Sampling strategy

Fieldwork was performed and aimed to collect six representative samples from geologic units, particularly the units that represent the water-bearing formation. A total of six samples were collected from the subsurface water wells at different depths. During the fieldwork, the location of these samples was registered using Global Positioning System (GPS). Detailed data is provided in Table 1.

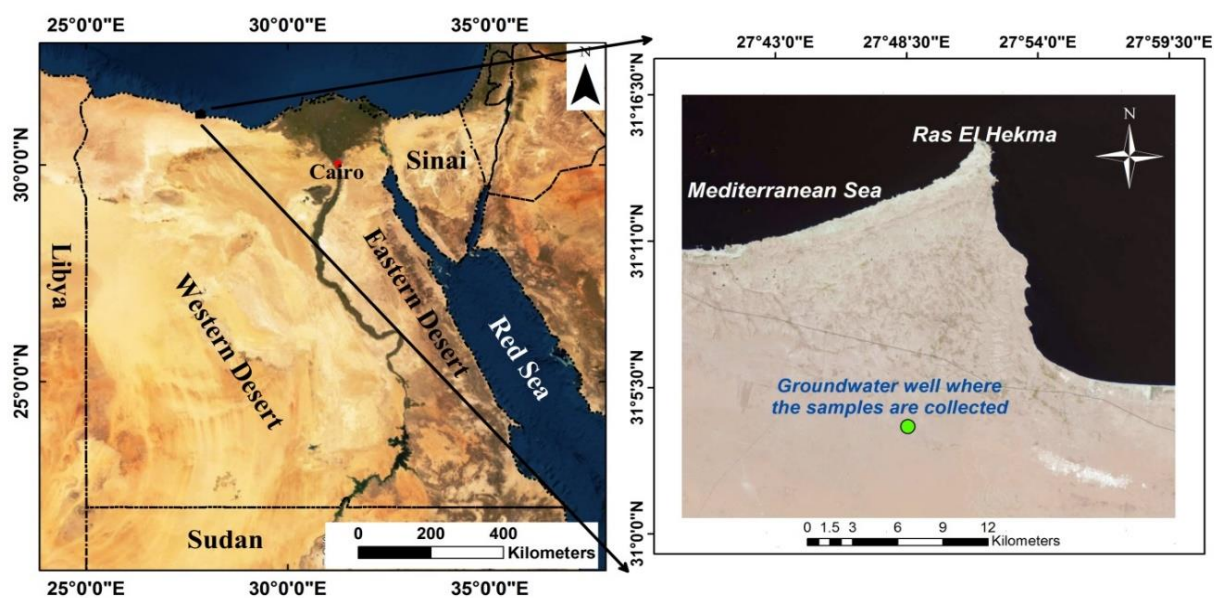


Fig. (1): Location map of the study area

Table (1): Data of the collected surface samples at different depths

Sample no.	Rock type	Area	Geologic Age	Remarks
1	Calcareous mudstone		Quaternary	Sample from the subsurface at a depth of 5 m
2	Limestone		Middle Miocene	Sample from the subsurface at a depth of 15 m
3	Limestone	Northwestern Coast,	Middle Miocene	Sample from the subsurface at a depth of 55 m
4	Limestone	Ras El Kekma	Middle Miocene	Sample from the subsurface at a depth of 71 m
5	Sand		Lower Miocene	Sample from the subsurface at a depth of 90 m
6	Sand		Lower Miocene	Sample from subsurface at depth 96 m

2.4. Sample preparation for neutron activation analysis (NAA)

First, the rock samples were crushed using an agate mortar to ensure homogeneity. Then, the samples were divided into two sets. The first set was prepared for the NAA to obtain the short-lived isotopes, while the second set was processed for the long-lived isotopes. The weights of the samples studied were collected in two groups, ranging from 150 to 300 mg. A set of samples were captured individually in polyethylene vials and then labeled. Similarly, the samples of the second set were separated into two groups and each group was inserted in an aluminum cup, which was sealed for long-lived isotope irradiation [2].

2.5. Analytical technique (NAA)

NAA was widely applied to determine the elemental composition of rock samples. The pneumatic rabbit system in the neutron activation laboratory of the second Egyptian research reactor (research reactor ETRR-2) was used for short irradiation. Each sample of the first group was irradiated for one minute, as well as the reference material. The thermal neutron flux of the short irradiation beam is $3.2 \times 10^{11} \text{ cm}^{-2} \text{ s}^{-1}$. After a short decay time of 2 to 5 min, the irradiated samples were measured with a high-purity germanium (HPGe) detector to determine the induced radioactivity. The two aluminum capsules containing the second group of samples and the reference material were irradiated for 33 min with a heat flux of about $1.33 \times 10^{14} \text{ cm}^{-2} \text{ s}^{-1}$ in (ETRR-2). After different decay times, the irradiated samples together with the reference material were measured with an HPGe detector [3].

The short-irradiated samples were allowed to decay for about two minutes and then counted for five minutes. After a one-hour decay period, the samples were counted again for 15 minutes intervals. In this way, isotopes with long half-lives can be detected for up to several hours. The long-irradiated samples were counted for 30 min after a cooling time of five to seven days and for two hours after a cooling time of

8-10 days to detect isotopes with half-lives of days to years. Samples and reference materials were analyzed using gamma-vision software and concentrations were determined using the relative standardization method. To carry out relative standardization, the sample and standard are irradiated together with neutrons, and the resulting radiation is measured using a detector. The intensity of the radiation from the sample is compared to that of the standard, and the composition of the sample can be calculated based on this comparison. This method is useful because it allows for the analysis of samples with unknown compositions, as long as a suitable standard is available. However, it is important to ensure that the conditions of the irradiation and measurement are consistent between the sample and standard, as any differences could affect the accuracy of the analysis. Additional detailed descriptions can be found in refs [33-38]. Induced radioactivity was measured using an N-type HPGe detector, model Comp-100.250-S, manufactured by (EG &G ORTEC) with associated electronics and a computer-based multichannel analyzer. The detector has a relative efficiency of 100% at 1332 keV and a FWHM of 2.1 keV and 0.875 keV at 1332 keV and 122 keV, respectively [2].

2.6. Quality control

The comparative method of NAA for the measurement of elements has been implemented. For this purpose, the quality of the measurements was weighted using a set of reference materials (IAEA-Soil-7). The samples and the reference-certified material were irradiated at the same conditions. The abundances of the certified and measured values of IAEA Soil- 7 are shown in Table S1 (supplementary materials). The relative error of the certified and measured abundances of the determined elements ranged from 5 to 25%. The results of the certified and measured abundances for the certified reference material are plotted and illustrated in Figure 2.

It can be seen from the figure that there is a good agreement between the abundances of the certified and measured elements. This agreement proves the accuracy of the measurements.

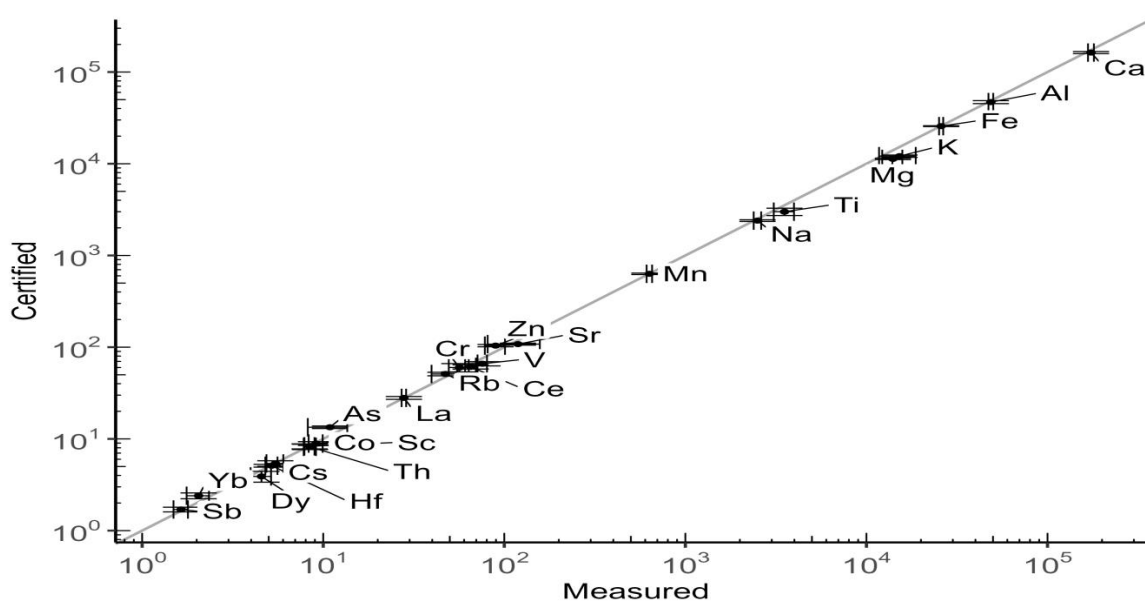


Fig. (2): log transformation of abundances of the certified and measured IAEA-Soil-7 CRM

2.7. Enrichment extent

2.7.1. Enrichment factor (EF)

Metal enrichment can be determined from the enrichment factor, as EF indicates the properties of the elements. Some elements can be used as reference elements to normalize the results and determine the degree of enrichment. For instance, Fe, Al, Sc, Ti, Mn, V, and Co can be used as normalizers. In the present work, EF was calculated using Fe as the reference element because Fe generally has a relatively high natural concentration and therefore is not expected to be significantly enriched in rocks. In addition, Fe was used for geochemical normalization because of its conservative geochemical behavior [39]. There is a large body of work addressing the calculations of EF in the literature [4, 40-46]. The (EF) is calculated using equation (1):

$$EF = (C_x/C_{Fe})_{sample}/(C_x/C_{Fe})_{reference} \quad (1)$$

where $(C_x/C_{Fe})_{sample}$ is the ratio between the abundance of elements in the sample and the abundance of Fe in the sample. While $(C_x/C_{Fe})_{reference}$ is the ratio of the corresponding element in the upper continental crust UCC abundance to Fe abundances reported by Rudnick and Gao [45].

2.7.2. Statistical data analysis

The normal distribution of the data was checked with the Shapiro-Wilk test [46]. The entire set of elements was analyzed with 95% probability and ($p \leq$

0.05). Analysis of variance (ANOVA) was performed. Descriptive statistics were calculated and provided. The intercorrelation coefficients were extracted and plotted. The ratio indicators and discrimination diagram were given to provide further information on the provenance and classification of rocks. The R software statistical package was used for all statistical analyses of the chemical data, including the infographics [47, 48].

3. RESULTS AND DISCUSSION

3.1. Elemental abundances and inter-correlation

A total of six rock samples were analyzed using NAA in terms of elemental composition collected at different depths. The descriptive statistics of abundances (mg/kg) of the determining of a total of 17 elements are given in Table 2. The obtained results were compared with the corresponding values from the literature by Rudnick and Gao [47] for the upper continental crust (UCC), Taylor and McLennan [51] for Post Archean Australia Shale (PAAS), Gromet, et al. [52] for the North American shale composite (NASC), and Kabata-Pendias [34] for the world average soil (WSA), respectively.

The average values \pm standard error (SE) were calculated and tabulated in Table 2. Considerable abundances of the mean values of Ca at all depths were found to be 255483 ± 69614 mg/kg. Contrariwise, the minimum values were noticed for Sb to be 0.18 ± 0.01 mg/kg. Specifically, the highest abundance of Ca was found at a depth of 71 m to be 399000 mg/kg, while the lowest

value at 90 m was to be 25700 mg/kg. The abundances of Ca were compared with those published in the literature and it is obvious that Ca has high amounts over UCC (25657 mg/kg), PAAS (9291 mg/kg), and NASC (25900 mg/kg), respectively. The descending order of the abundances of the elements can be given as follows: Ca>Mg>Al>Fe>K>Ti>Na>Sr>Mn>V>Ce>La>Co>Hf>Th>Sc>Sb.

In addition, the abundances of the determining elements were normalized to the corresponding value of the upper continental crust (UCC) by [47]. as clearly illustrated in Figure 3. Only two types of rocks were

plotted as the third one is only one representative sample. The figure depicts that almost all the elements' abundance is lower than the corresponding values in UCC, except for Ca, Sr, and Mg in the plot of limestone. The high abundances of Ca and Mg indicate that the sedimentary rocks are limestone. The limestones are primarily formed by the lithification of calcium carbonate sediments, which involves various steps beginning with changes in grain mineralogy and includes adding concentric coatings to grains, selective dissolution of matrix and/or grains, precipitation of mineral cement in pore spaces, and may end in recrystallization [54].

Element	Mean± SE	Median± MAD	Min-Max	Skew	Kurtosis	CV%	Statistic	p-value	UCC	PAAS	NASC	WSA
Na	1984±537	1835±1248	719-4180	0.5	-1.45	66	0.901	0.378	24258.57	9644.08	1370	ND
Mg	13973±4715	11150±4833	5860-36800	1.17	-0.38	83	0.719	0.010	14953.85	13265.5	1334	ND
Al	11227±4068	8850±8555	2600-28800	0.7	-1.2	89	0.865	0.208	81510.71	100036	67000	ND
K	6040±1762	6500±3573	117-12700	0.12	-1.41	71	0.971	0.897	23244.16	30715.5	ND	ND
Ca	255483±6961 4	329500±10081 7	25700- 399000	-0.46	-1.95	67	0.789	0.046	25657.49	9291.01	25900	ND
Sc	2±1	2±1	1-5	0.68	-1.19	71	0.893	0.337	14	16	30	11.7
Ti	2049±491	2270±875	371-3900	0.09	-1.38	59	0.936	0.624	3835.79	5993.43	4196	7038
V	26±5	25±11	13-45	0.44	-1.36	45	0.941	0.665	97	150	130	129
Mn	128±23	126±75	68-191	0.03	-2.2	43	0.846	0.147	774.46	ND	ND	488
Fe	8008±2261	6520±5434	2420-16200	0.38	-1.82	69	0.909	0.431	39175.06	50523.4	14100	ND
Co	4±1	4±3	1-9	0.35	-1.69	76	0.908	0.424	17.3	23	26	11.3
Sr	540±65	618±31	241-660	-0.99	-0.81	29	0.754	0.022	320	200	142	175
Sb	0.18±0.01	0.19±0.01	0.14-0.21	-0.35	-1.81	17	0.859	0.184	0.4	ND	7.3	0.67
La	7±2	7±5	3-14	0.32	-1.6	61	0.942	0.674	31	38	31.1	27
Ce	17±4	17±11	5-32	0.24	-1.55	60	0.939	0.651	63	80	66.7	56.7
Hf	3±1	3±1	1-5	0.04	-1.39	46	0.931	0.587	5.3	5	6.3	6.4
Th	2.1±0.3	2.32±0.35	1-3	-0.56	-1.34	30	0.886	0.296	10.5	14.6	12.3	9.2

UCC = upper continental crust [45], PAAS = Post Archean Australia Shale PAAS Taylor and McLennan [49], NASC = North American shale composite [50], WAS = world average soil [51], ND = not detected.

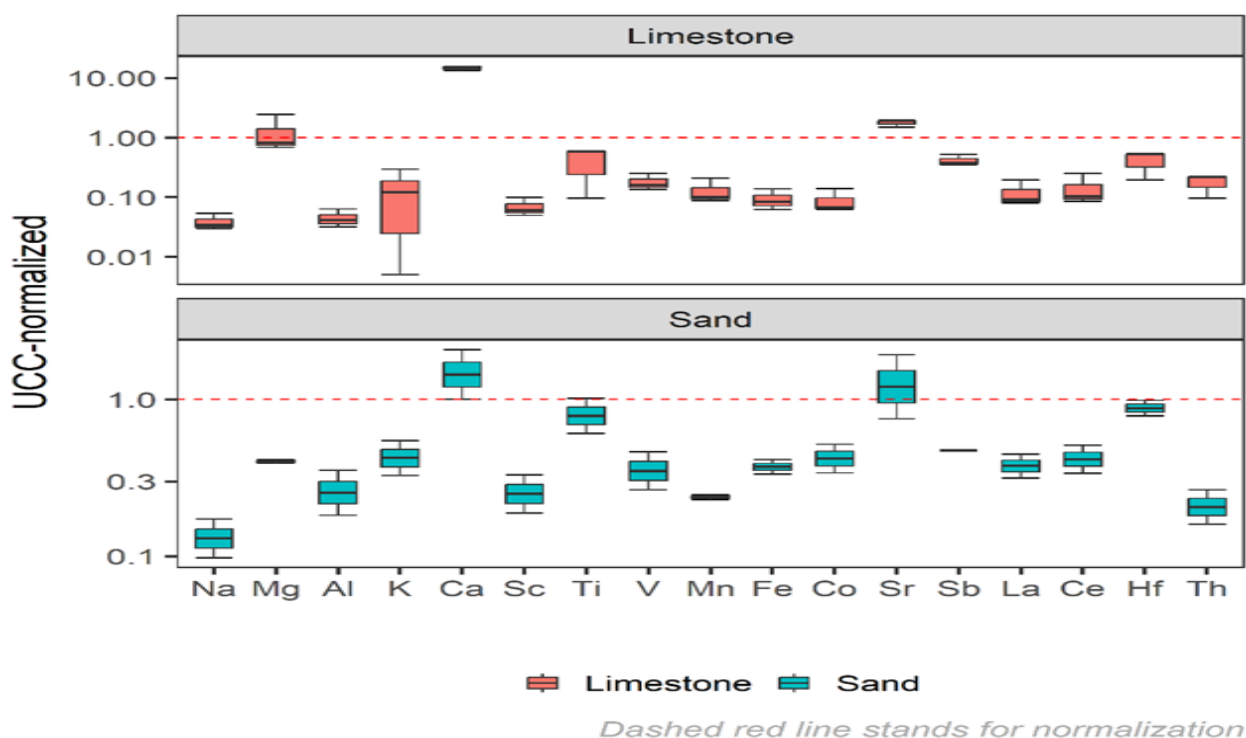


Fig. (3): boxplot illustrating the normalized abundances to UCC

The normality test was carried out using Shapiro-Wilk [48], and the results of the test revealed that almost all the elements are normally distributed except Mg, Ca, and Sr ($p < 0.05$). The two-way analysis of variance ANOVA was carried out and the results show that the null hypothesis is rejected ($p < 0.0001$) in terms of elements. While the null hypothesis is accepted in terms of depths ($p = 0.533$) and this means that there is no significant statistical difference in terms of the collected samples. The distribution of the elements' abundance shows moderate variations. The coefficient of variation (CV %) ranges from 17 to 89 % for Sb and Al, respectively. CV% values suppose considerable variations in the mean values of the abundances of the samples. Similarly; the values of skewness and kurtosis range from -0.99 (Sr) to 1.17 (Mg) and from -2.2 (Mn) to -0.38 (Mg), respectively.

Based on the fact that high values of CV ($> 75\%$), positive skewness (> 0), and kurtosis (> 3) are likely to indicate the non-normal distribution [55]. The results obtained agree well with the results of the normality test, except for Sr. This peculiarity can be explained by the strong variations in the abundances of Sr at different depths, which in turn leads to the appearance of outliers and tends to create separate groups.

The correlation coefficients were extracted based on the Pearson method and clustered using the Ward

method. The strongest correlation coefficients were calculated for some pairs and in particular; (Al:Sc), (La:Ce), and (Na:Co) (≈ 0.99). In addition, with a correlation coefficient higher than 0.98 the pairs for (Na:Al), (Co:La), (Al:Co), (Sc:Co), (Na:Sc), and (Sc:La) were noticed. The results revealed that Ca, Mg, and in part Sr, have a negative correlation with other elements. This outcome can be attributed to the elevated amounts of these elements relative to others. The correlation matrix was plotted and illustrated as shown in Figure 4. The figure was plotted based on the cluster method of highly correlated elements and the cold color refers to positive correlation, while the hot one stands for negative correlation.

To extract more information about the relationship of abundances of the elements via depths, a plot illustrating the behavior of the abundances at different depths Figure 5. At first glance, the findings prove the fact that regardless of the type of rocks the abundances of elemental compositions are different at different depths [5]. For instance, all the identified elements except Sb, Th, Hf, Ti, Mg, K, and Ca behaved similarly at depth. Their abundances were remarkably different within depth. The abundance of Ca is almost constant via depth except at 90 and 96 m depths. Mostly because the last two samples are limestone. The obtained results are consistent with the description of the samples in Table 1.

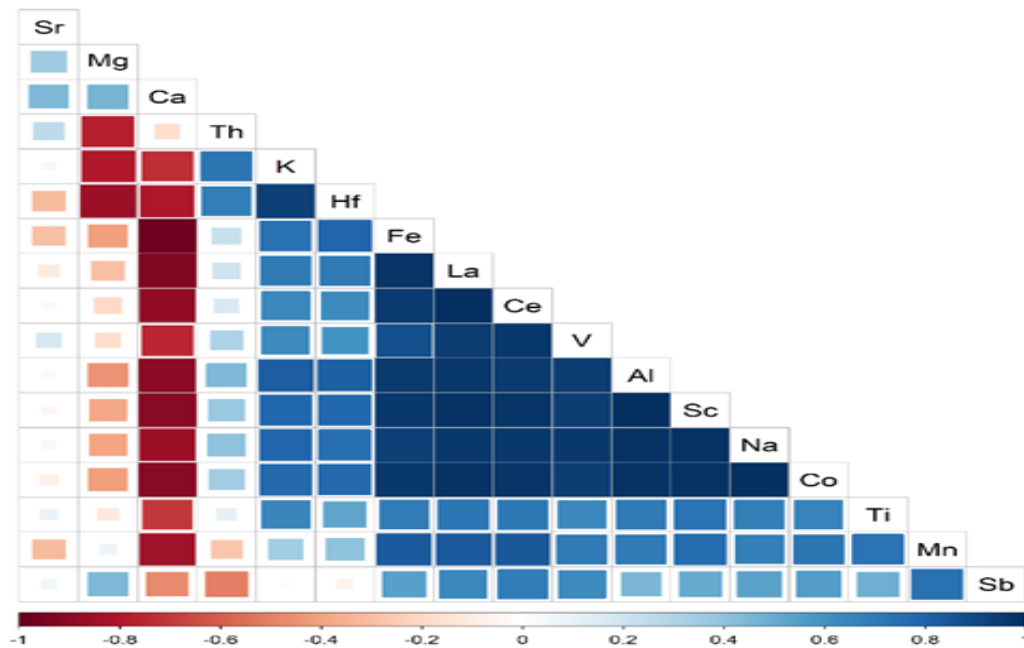


Fig. (4): the correlation matrix clustered by the Ward method

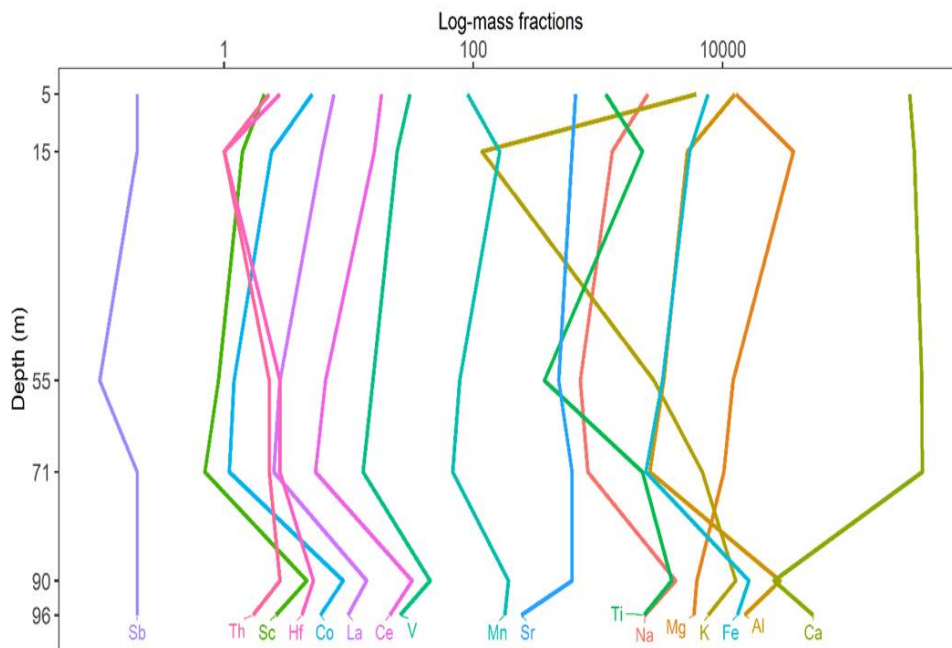


Fig. (5): log-transformed abundances of the elements at different depths

3.2. The provenance of sedimentary rocks

The provenance of the sedimentary rocks was examined based on the obtained geochemical data. The discrimination diagram of La – Sc – Th was plotted as clearly shown in Figure 6. The corresponding values from the literature by Rudnick and Gao [45] for UCC, Gromet, Haskin, Korotev, and Dymek [52] for NASC,

[51] for PAAS, and Kabata-Pendias [55] for WSA, respectively. It is obvious from the figure that most of the samples are located in the vicinity of UCC and WSA. It is obvious from the figure that most of the samples are located in the vicinity of UCC and WSA. According to Bhatia and Crook [56], the origin of the rocks is mainly continental island arc, except for the samples at 55 and 71

m depths tend to the active and passive continental margins. These findings prove that there is a significant association of clay, silt, sand, and gravel from the mixed source [57].

Another discrimination diagram was developed by Blatt, et al. [58] and used to differentiate between sandstones. The discrimination diagram of $Fe_2O_3 + MgO - Na_2O - K_2O$ is plotted and illustrated in Figure 7. Nearly most of the samples from the well were found in the field of lithic sandstone. The results of the figure demonstrate how accurately the analytical procedure was used.

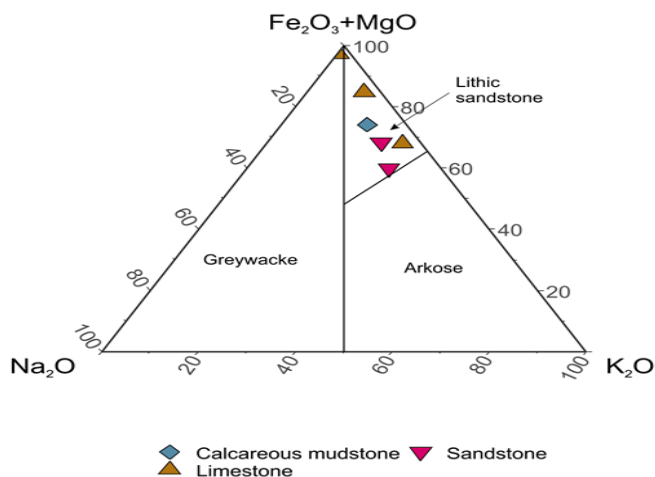


Fig. (7): the discrimination diagram of $Fe_2O_3 + MgO - Na_2O - K_2O$

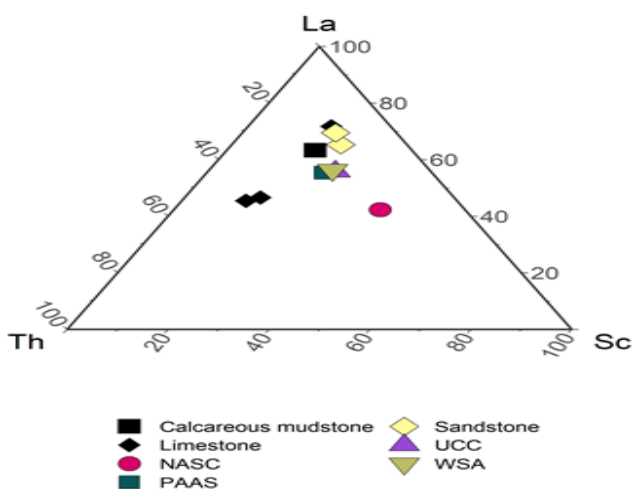


Fig. (6): the ternary diagram illustrating the relation of La - Sc - Th [39] for tectonic setting discrimination. The results compared with the corresponding values from the literature

3.3. Observations of enrichment extent

The enrichment factor (EF) was used to assess to what extent the elements are enriched. The obtained results of EF were plotted and illustrated as shown in Figure 8. The figure depicts that the EF of Ca is remarkable at depths 5, 15, 55, and 71 m. Additionally, the EF of Mg and Sr is significant at almost the same depths. The average value of EF was noticed to be 10.9 with a minimum value of 1.8 at 90 m depth and a maximum value of 23.9 at 71 m depth. According to the interpretation of the different classes and criteria of EF, from strong to extremely strong enrichment was calculated for Mg, Sr, and Ca. The significant amounts of Ca can be explained by the nature of limestone. The interpretation and the enriched elements are provided in the inset table in Figure 8.

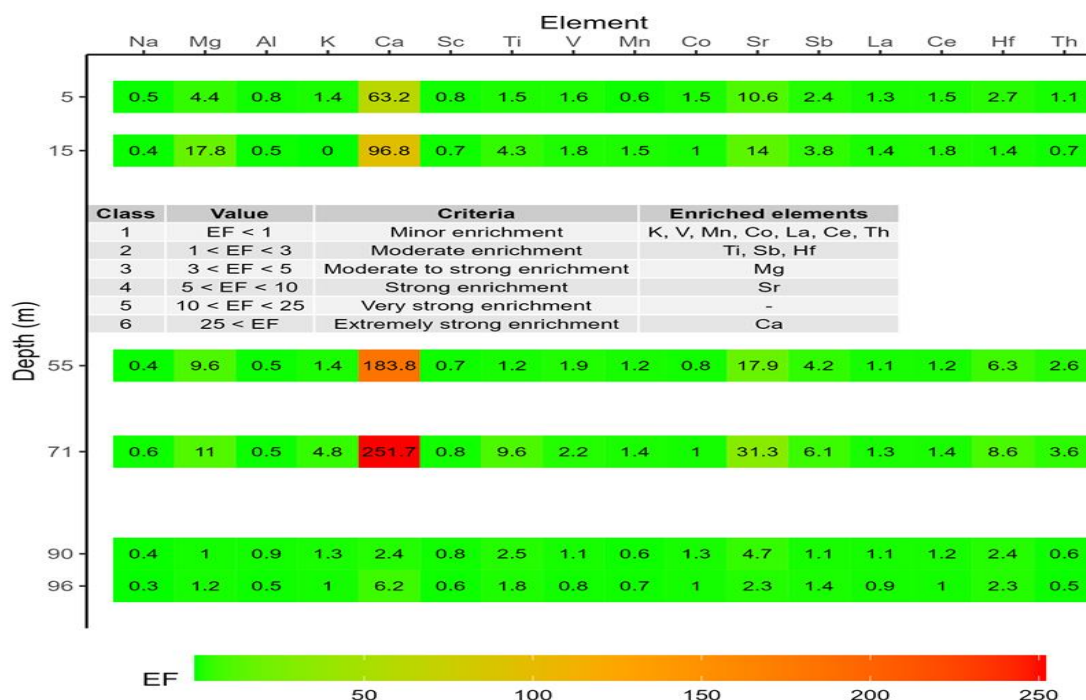


Fig. (8): the distribution pattern of the enrichment factor of the obtained elements at different depths

3.4. Findings of hierarchal clustering analysis (HCA)

The clustering method is about dissimilarities or distances between objects to form clusters. The hierarchical method is usually described by a graphical output, called a dendrogram, which shows this hierarchical cluster structure [42]. Hierarchical clustering analysis is the most common type of hierarchical clustering, where observations are linked into groups based on their similarity or dissimilarity. More details about the various functions and applications are published by [60-63].

HCA proceeded based on the geochemical data of the determining elements (R Core Team, 2020). Specifically, the package “cluster” for agglomerative nesting AGNES was used. To obtain information about the appropriate metric for reproducing the similarity matrix and the correct method for clustering, the best-known methods for clustering were calculated in terms of agglomerative coefficient, and the larger the coefficient is, the better the method fits the data set. Therefore, the Manhattan metric for creating the

similarity or dissimilarity matrix and the full method for clustering were implemented.

The agglomerative coefficients (AC) of the different methods were 0.38, 0.20, 0.53, 0.52, and 0.41 for average, single, complete, Ward, and weighted, respectively. Based on the calculated AC, the highest value for the complete clustering method was obtained. Based on the extracted information about the metric and method of clustering, the agglomerative hierarchical clustering was plotted and illustrated in Figure 9. The figure depicts 2 groups in terms of the type of rocks that are linked based on their common geochemical features. The groups are namely, the 1st cluster contains types #1, 5, and 6. Referring to Table 1, these types are Calcareous mudstone, and sand, respectively. On the other hand, the 2nd cluster includes three types and all of them are limestone.

The obtained results of HCA demonstrate the high precision and accuracy of neutron activation analysis in rock analysis in terms of elemental composition. Moreover, the analysis of HCA resulted in two clusters and each cluster contains rocks with common geochemical characteristics.

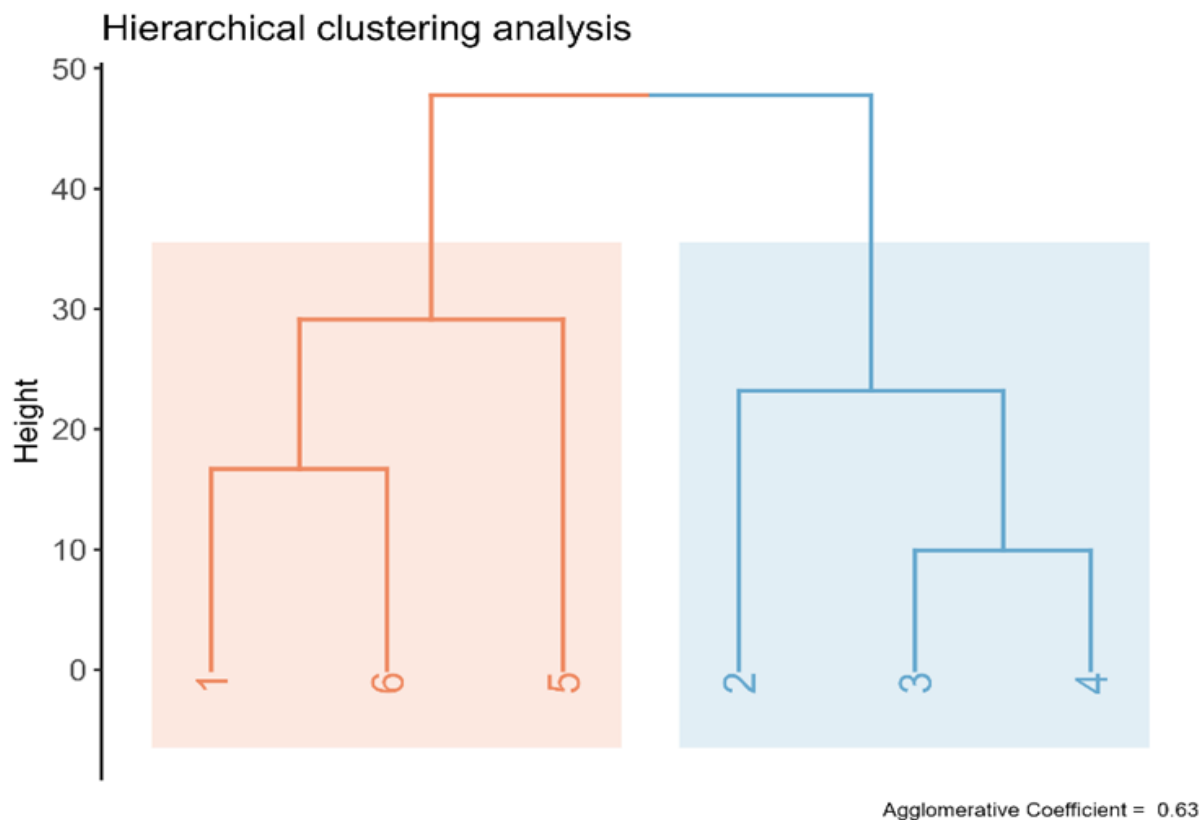


Fig. (9): hierarchical clustering analysis depicting two clusters

CONCLUSION

The main goal of the current study was to determine the concentrations of the elements in six subsurface rock samples from North-western Coast, of Ras El-Hekma – Egypt. The concentrations of a total of 17 elements were measured at different depths using NAA. The results show considerable amounts of Ca at almost all depths. The highest and lowest concentrations of Ca were found at 71 and 90 m depths, respectively. Furthermore, the results were normalized to the corresponding values of UCC, and the normalized abundances show that Ca and Sr have remarkable concentrations. The normality test shows that there is no significant statistical difference in terms of the depths of the samples. Based on the discriminant diagrams, the research has shown that the origin of the elements is mainly continental island arc, except samples 55 and 71 m depths tend to the active and passive continental margins. Likewise, the ratio indicator Co-Th shows that most of the samples are in the vicinity of the calc-alkaline series. The enrichment factor was computed and classified as strong to extremely strong for Sr and Ca, respectively. These results contribute significantly to our understanding of the geochemistry of the rocks in the study area and provide a basis for background values of the elemental composition of the rocks. In addition, the results obtained become a scientific judgment on whether measures should be taken to ensure the quality of the water supply for humans and the environment.

A Dispute of Interest:

There was no conflict of interest disclosed by the authors.

Information About Data Availability:

The data performed at the Egyptian Atomic Energy Authority.

Funding

No funding was provided by any organization or funding agency to any author for the implementation of this research or the publication of the paper.

REFERENCES

- [1] Manahan, S.(2017), Environmental chemistry, Tenth edition; CRC Press: Boca Raton,; pp. 1-784.
- [2] Massoud A, Fatma S, Abdou & Mohamed Yousif, (2023) Evaluation of mineral compositions of surface and subsurface rock samples by neutron activation analysis. *Int J Environ Anal Chem* 103:528-545.
[https://doi.org/ 10.1080/ 03067319.2020.1862095](https://doi.org/10.1080/03067319.2020.1862095)
- [3] Bhakta, S.; Rout, T.K.; Karmakar, D.; Pawar, C.; Padhy, P.K. (2022) Trace elements and their potential risk assessment on polar ecosystem of Larsemann Hills, East Antarctica. *Polar Science*, 31:100788,
<https://doi.org/10.1016/j.polar.2022.100788>.
- [4] Badawy, W.M.; Ghanim, E.H.; Duluiu, O.G.; El Samman, H.; Frontasyeva, M.V. (2017) Major and trace element distribution in soil and sediments from the Egyptian central Nile Valley. *Journal of African Earth Sciences*, 131:53-61,
[doi:10.1016/j.jafrearsci.2017.03.029](https://doi.org/10.1016/j.jafrearsci.2017.03.029).
- [5] Lipp, A.G.; Shorttle, O.; Syvret, F.; Roberts, G.G. (2020) Major Element Composition of Sediments in Terms of Weathering and Provenance: Implications for Crustal Recycling. *Geochemistry, Geophysics, Geosystems* 21: e2019GC008758,
<https://doi.org/10.1029/2019GC008758>.
- [6] McLennan, S.M.; Hemming, S.; McDaniel, D.K.; Hanson, G.N. (1993) Geochemical approaches to sedimentation, provenance, and tectonics. In *Processes Controlling the Composition of Clastic Sediments*, Johnsson, M.J., Basu, A., Eds.; Geological Society of America.
- [7] Philpotts, A.R.; Ague, J.J. (2022) *Principles of Igneous and Metamorphic Petrology*, 3 ed.; Cambridge University Press: Cambridge.
- [8] Blatt, H.; Tracy, R.; Owens, B. *Petrology: (2006) Igneous, Sedimentary, and Metamorphic*; W. H. Freeman.
- [9] Kovalenko, V.I.; Kozlovsky, A.M.; Yarmolyuk, V.V. (2009) Trace element ratios as indicators of source mixing and magma differentiation of alkali granitoids and basites of the Haldzan-Buregtey massif and the Haldzan-Buregtey rare-metal deposit, western Mongolia. *Petrology* 17:158-177,
[doi:10.1134/S0869591109020040](https://doi.org/10.1134/S0869591109020040).
- [10] López, P.; Navarro, E.; Marcé, R.; Ordoñez, J.; Caputo, L.; Armengol, J. (2006) Elemental ratios in sediments as indicators of ecological processes in Spanish reservoirs. *Limnetica*, 25, 499-512,
[doi:10.23818/limn.25.34](https://doi.org/10.23818/limn.25.34).
- [11] Dietrich, R.V.; Skinner, B.J. (1979) *Rocks and Rock Minerals*; Wiley:.

- [12] Buccianti, A. (2013) Is compositional data analysis a way to see beyond the illusion? *Computers & Geosciences* 50:165-173, <https://doi.org/10.1016/j.cageo.2012.06.012>.
- [13] Aitchison, J. The (1982) *Statistical Analysis of Compositional Data*. Journal of the Royal Statistical Society. Series B (Methodological) 44:139-177.
- [14] Ayman Massoud and Hazem H. Mahmoud, (2023) Performance appraisal of a cross-linked polymer prepared by gamma radiation for the removal of copper and its binding mechanism, *International Journal of Polymer Analysis and Characterization*, 28:12–31. <https://doi.org/10.1080/1023666X.2022.2138136>
- [15] Massoud A. and Mahmoud H.H., (2023), Recovery of Zn(II) from Simulated Liquid Waste Using Poly(Vinyl Alcohol-Acrylamide) Synthesized by Gamma Radiolysis Method. *Journal of Polymers and the Environment*, 31:4960–4971. <https://doi.org/10.1007/s10924-023-02910-1>
- [16] Massoud & S. A. Waly, (2014) Preparation and characterization of poly (acrylic acid-dimethylaminoethylmethacrylate) as amphoteric exchange resin and its adsorption properties, *Colloid and Polymer Science*, 292(12):3077. [DOI 10.1007/s00396-014-3335-4](https://doi.org/10.1007/s00396-014-3335-4)
- [17] Massoud A. & Mansor H. H., (2017) Evaluation of hybrid polymeric resin containing nanoparticles of iron oxide for selective separation of In (III) from Ga (III) *J Inorg Organomet Polym*, 27:1806,. [DOI 10.1007/s10904-017-0645-2](https://doi.org/10.1007/s10904-017-0645-2)
- [18] Massoud A., Waly S. A., and Abou El-Nour F., (2017) Removal of U (VI) from simulated liquid waste using synthetic organic resin, *Radiochemistry*, 59(3) 272. [DOI: 10.1134/S1066362217030092](https://doi.org/10.1134/S1066362217030092)
- [19] Massoud A., Ahmed M Masoud, WM Youssef, (2019) Sorption characteristics of uranium from sulfate leach liquor by commercial strong base anion exchange resins, *Journal of Radioanalytical and Nuclear Chemistry*, 322:1065. <https://doi.org/10.1007/s10967-019-06770-9>
- [20] Massoud A., S. B. Challan & Nabila Maziad, (2021) Characterization of polyvinylpyrrolidone (PVP) with technetium-99m and its accumulation in mice, *Journal of Macromolecular Science, Part A*, 58(6):408-418. <https://doi.org/10.1080/10601325.2021.1873070>.
- [21] Massaoud A.A., H.A. Hanafi, T. Siyam, Z.A. Saleh, F.A., Ali, (2008) Separation of Ga(III) from Cu(II), Ni(II) and Zn(II) in aqueous solution using synthetic polymeric resins, *Cent. Eur. J. Chem.*, 6(1):39-45. <https://doi.org/10.2478/s11532-007-0054-4>
- [22] Ayman Massoud, F Abou El-Nour, H Killa, U Seddik, (2010), Chromatographic separation of In (III) from Cd (II) in aqueous solutions using commercial resin (Dowex 50W-X8), *Cent. Eur. J. Chem.*, 8(3): 696-701. <https://doi.org/10.2478/s11532-010-0041-z>
- [23] Rachel L White, Cale M White, Hulusi Turgut, A Massoud, Z Ryan Tian, Comparative studies on copper adsorption by graphene oxide and functionalized graphene oxide nanoparticles, *Journal of the Taiwan Institute of Chemical Engineers*, 85, 2018, 18-28. <https://doi.org/10.1016/j.jtice.2018.01.036>
- [24] Challan, S.B., Massoud, A., (2017) Radiolabeling of graphene oxide by Technetium-99m for infection imaging in rats, *J Radioanal Nucl Chem* 314:2189-2199. <https://doi.org/10.1007/s10967-017-5561-y>
- [25] Massoud, A., Rizk, H.E. & Attallah, M.F., (2021) Selective separation of Y(III) from Sr(II) using hybrid polymer: synthesis, characterization, batch and column study, *Polym. Bull.* 78:7053–7069. <https://doi.org/10.1007/s00289-020-03479-8>
- [26] Challan SB, Marzook FA, Massoud A. (2020) Synthesis of radioiodinated carnosine for hepatotoxicity imaging induced by carbon tetrachloride and its biological assessment in rats, *Radiochim Acta*, 108(5):397– 408,. <https://doi.org/10.1515/ract-2019-3162>
- [27] Motaleb M. A., M. El-Tawoosy, S. B. Mohamed, I. H. Borei, H. M. Ghanem, and A. A. Massoud, (2014) 99m Tc-labeled teicoplanin and its biological evaluation in experimental animals for detection of bacterial infection, *Radiochemistry*, 56(5):544-549. <https://doi.org/10.1134/S1066362214050154>
- [28] Safaa B. Challan, A. A. Massoud, M. El Tawoosy, M. A. Motaleb, I. H. Borei and HMG. (2018), 99mTc-Labeled Erythrocin and Biological Evaluation in Mice for Detection of Bacterial Infection, *Asian J Phys Chem Sci.*, 5(2):2456-7779,. [DOI:10.9734/AJOPACS/2018/40170](https://doi.org/10.9734/AJOPACS/2018/40170)

- [29] Mohamed Z. Twfiq, Fardous M. Zarif, A. Massoud, and Ayman M. Al-Temamy (2021) Determination the Petrophysical and Natural Radioactivity Properties of Nubian Sandstone Aquifer at the Area of Northwest El Ain Village, Sharq El-Oweinat Area, Southwestern, Asian Journal of Environment & Ecology, 15(4):37-55 Article no.AJEE.70730, [DOI:10.9734/AJEE/2021/v15i430236](https://doi.org/10.9734/AJEE/2021/v15i430236)
- [30] Frontasyeva, M.V. (2011) Neutron activation analysis in the life sciences. Physics of Particles and Nuclei, 42:332-378, [doi:10.1134/S1063779611020043](https://doi.org/10.1134/S1063779611020043).
- [31] Yousif, M.; Bubenzer, O. (2013) An integrated approach for groundwater assessment at the Northwestern Coast of Egypt (Ras El Hekma area): a case study. Environmental Earth Sciences, 69:2227-2246, [doi:10.1007/s12665-012-2052-x](https://doi.org/10.1007/s12665-012-2052-x).
- [32] Conoco. 1986, Geologic Map of Egypt.
- [33] Massoud, A.; Farid, O.M.; Maree, R.M.; Allan, K.F.; Tian, Z.R. An improved metal cation capture on polymer with graphene oxide synthesized by gamma radiation. Reactive and Functional Polymers 2020, 151, 104564, <https://doi.org/10.1016/j.reactfunctpolym.2020.104564>.
- [34] Ayman Massoud & Hazem H. Mahmoud (2023) Performance appraisal of a cross-linked polymer prepared by gamma radiation for the removal of copper and its binding mechanism, International Journal of Polymer Analysis and Characterization, 28(1):12-31, [DOI: 10.1080/1023666X.2022.2138136](https://doi.org/10.1080/1023666X.2022.2138136)
- [35] Ghamry, M.A., Abido, A.M.N. & Massoud, A. (2023) Remediation of Cs-134 from liquid solution by synthesized poly(vinyl alcohol-acrylamide) blended with CuO nanoparticles. J Radioanal Nucl Chem 332, 3635–3649 <https://doi.org/10.1007/s10967-023-09042-9>
- [36] Bode, P.; Greenberg, R.R.; De Nadai Fernandes, E.A. (2009) Neutron Activation Analysis: A Primary (Ratio) Method to Determine SI-Traceable Values of Element Content in Complex Samples., 63:3 <https://doi.org/10.2533/chimia.2009.678>.
- [37] Greenberg, R.R.; Bode, P.; De Nadai Fernandes, E.A. (2011) Neutron activation analysis: A primary method of measurement. Spectrochimica Acta Part B: Atomic Spectroscopy, 66:193-241, [doi:https://doi.org/10.1016/j.sab.2010.12.011](https://doi.org/10.1016/j.sab.2010.12.011).
- [38] Bode, P. (2017) Neutron Activation Analysis (NAA). In Neutron Methods for Archaeology and Cultural Heritage, Kardjilov, N., Festa, G., Eds.; Springer International Publishing: Cham, pp. 209-219.
- [39] Lv, J.; Liu, Y.; Zhang, Z.; Zhou, R.; Zhu, Y. (2015) Distinguishing anthropogenic and natural sources of trace elements in soils undergoing recent 10-year rapid urbanization: a case of Donggang, Eastern China. Environmental Science and Pollution Research, 22:10539-10550, [doi:10.1007/s11356-015-4213-4](https://doi.org/10.1007/s11356-015-4213-4).
- [40] Abraham, G.M.S.; Parker, R.J. (2008) Assessment of heavy metal enrichment factors and the degree of contamination in marine sediments from Tamaki Estuary, Auckland, New Zealand. Environmental Monitoring and Assessment, 136:227-238, [doi:10.1007/s10661-007-9678-2](https://doi.org/10.1007/s10661-007-9678-2).
- [41] Reimann, C.; de Caritat, P. (2005) Distinguishing between natural and anthropogenic sources for elements in the environment: regional geochemical surveys versus enrichment factors. Science of the Total Environment, 337:91-107. [doi:https://doi.org/10.1016/j.scitotenv.2004.06.011](https://doi.org/10.1016/j.scitotenv.2004.06.011).
- [42] Badawy, W.M.; El-Taher, A.; Frontasyeva, M.V.; Madkour, H.A.; Khater, A.E.M. (2018) Assessment of anthropogenic and geogenic impacts on marine sediments along the coastal areas of Egyptian Red Sea. Appl Radiat Isot, 140:314-326, [doi:10.1016/j.apradiso.2018.07.034](https://doi.org/10.1016/j.apradiso.2018.07.034).
- [43] Badawy, W.M.; Dului, O.G.; Frontasyeva, M.V.; El-Samman, H.; Mamikhin, S.V. (2020) Dataset of elemental compositions and pollution indices of soil and sediments: Nile River and delta -Egypt. Data Brief, 28:105009, [doi:10.1016/j.dib.2019.105009](https://doi.org/10.1016/j.dib.2019.105009).
- [44] Ergin, M.; Saydam, C.; Baştürk, Ö.; Erdem, E.; Yörük, R. (1991) Heavy metal concentrations in surface sediments from the two coastal inlets (Golden Horn Estuary and İzmit Bay) of the northeastern Sea of Marmara. Chemical Geology, 91:269-285, [https://doi.org/10.1016/0009-2541\(91\)90004-B](https://doi.org/10.1016/0009-2541(91)90004-B).
- [45] Chen, C.W.; Kao, C.M.; Chen, C.F.; Di Dong, C. (2007) Distribution and accumulation of heavy metals in the sediments of Kaohsiung Harbor, Taiwan. Chemosphere 66:1431–1440, [doi:10.1016/j.chemosphere.2006.09.030](https://doi.org/10.1016/j.chemosphere.2006.09.030).

- [46] Badawy, W.M.; Dulu, O.G.; El Samman, H.; El-Taher, A.; Frontasyeva, M.V. (2021) A review of major and trace elements in Nile River and Western Red Sea sediments: An approach of geochemistry, pollution, and associated hazards. *Appl Radiat Isot*, 170:109595, [doi:10.1016/j.apradiso.2021.109595](https://doi.org/10.1016/j.apradiso.2021.109595).
- [47] Rudnick, R.L.; Gao, S. (2014) Composition of the Continental Crust. In *Treatise on Geochemistry*, Turekian, K.K., Ed.; Elsevier: Oxford, pp. 1-51.
- [48] Shapiro, S.S.; Wilk, M.B. (1965) An analysis of variance test for normality (complete samples). *Biometrika*, 52:591-611, [doi:10.1093/biomet/52.3-4.591](https://doi.org/10.1093/biomet/52.3-4.591).
- [49] R Core Team R: (2020) A language and environment for statistical computing. R Foundation for Statistical Computing, Vienna, Austria, <https://www.R-project.org/>.
- [50] Vojtech, J.; Farrow, C.M.; Erban, V. (2006) Interpretation of Whole-rock Geochemical Data in Igneous Geochemistry: Introducing Geochemical Data Toolkit (GCDkit). *Journal of Petrology*, 47:1255-1259, [doi:10.1093/petrology/egl013](https://doi.org/10.1093/petrology/egl013).
- [51] Taylor, S.R.; McLennan, S.M. (1985) The continental crust, its composition and evolution : an examination of the geochemical record preserved in sedimentary rocks; Oxford : Blackwell Scientific, p. 312.
- [52] Gromet, L.P.; Haskin, L.A.; Korotev, R.L.; Dymek, R.F. (1984) The "North American shale composite": Its compilation, major and trace element characteristics. *Geochimica et Cosmochimica Acta*, 48:2469-2482, [doi:10.1016/0016-7037\(84\)90298-9](https://doi.org/10.1016/0016-7037(84)90298-9).
- [53] Kabata-Pendias, A. (2011) Trace elements in soils and plants, 4 ed.; Boca Raton, p. 548.
- [54] Sanders, J.E.; Friedman, G.M. (1967) Chapter 5 Origin and Occurrence of Limestones. Work on this chapter commenced in the Department of Geology, Yale University, but was completed after the senior author became a Senior Research Associate, Columbia University. Contribution No.66-5 of the Department of Geology, Rensselaer Polytechnic Institute. In *Developments in Sedimentology*, Chilingar, G.V., Bissell, H.J., Fairbridge, R.W., Eds.; Elsevier 9:169-265.
- [55] Allajbeu, S.; Yushin, N.S.; Qarri, F.; Dulu, O.G.; Lazo, P.; Frontasyeva, M.V. (2016) Atmospheric deposition of rare earth elements in Albania studied by the moss biomonitoring technique, neutron activation analysis and GIS technology. *Environmental Science and Pollution Research*, 23:14087-14101, [doi:10.1007/s11356-016-6509-4](https://doi.org/10.1007/s11356-016-6509-4).
- [56] Bhatia, M.R.; Crook, K.A.W. (1986) Trace element characteristics of graywackes and tectonic setting discrimination of sedimentary basins. *Contributions to Mineralogy and Petrology*, 92:181-193, [doi:10.1007/BF00375292](https://doi.org/10.1007/BF00375292).
- [57] Badawy, W.; Frontasyeva, M.V.; Ibrahim, M. (2020) Vertical Distribution of Major and Trace Elements in a Soil Profile from the Nile Delta, Egypt. *Ecological Chemistry and Engineering S-Chemia I Inzynieria Ekologiczna S*, 27:281-294, [doi:10.2478/eces-2020-0018](https://doi.org/10.2478/eces-2020-0018).
- [58] Blatt, H.; Middleton, G.V.; Murray, R.C. (1980) *Origin of Sedimentary Rocks*; Englewood Cliffs, N.J. : Prentice-Hall.
- [59] Ashraf, A.; Saion, E.; Gharibshahi, E.; Kamari, H.M.; Yap, C.K.; Hamzan, M.S.; Elias, M.S. (2017) Distribution of Trace Elements in Core Marine Sediments of Coastal East Malaysia by Instrumental Neutron Activation Analysis. *Applied Radiation and Isotopes*, 122:96-105, [doi:10.1016/j.apradiso.2017.01.006](https://doi.org/10.1016/j.apradiso.2017.01.006).
- [60] Struyf, A.; Hubert, M.; Rousseeuw, P. (1997) Clustering in an Object-Oriented Environment. *Journal of Statistical Software*, 1:1-30, [doi:10.18637/jss.v001.i04](https://doi.org/10.18637/jss.v001.i04).
- [61] Kaufman, L.; Rousseeuw, P.J. (1990) Agglomerative Nesting (Program AGNES). In *Finding Groups in Data*; John Wiley & Sons: Hoboken, NJ, USA, pp. 199-252.
- [62] Kamanina, I.Z.; Badawy, W.M.; Kaplina, S.P.; Makarov, O.A.; Mamikhin, S.V. (2023) Assessment of Soil Potentially Toxic Metal Pollution in Kolchugino Town, Russia: Characteristics and Pollution. *Land* 12:439, <https://doi.org/10.3390/land12020439>.
- [63] Carlson, D.L. (2017) *Quantitative Methods in Archaeology Using R*; University of Cambridge, Cambridge, UK.,.